Advances in Radiation Oncology (2016) **1**, 281-289

advances
in radiation oncology

www.advancesradonc.org

Scientific Article

Priority-driven plan optimization in locally advanced lung patients based on perfusion SPECT imaging

Martha M. Matuszak PhD [a,b,*], Charles Matrosic MS [a,b], David Jarema [a], Daniel L. McShan [a], Matthew H. Stenmark MD [a], Dawn Owen MD [a], Shruti Jolly MD [a], Feng-Ming (Spring) Kong MD [c], Randall K. Ten Haken PhD [a]

[a] *Department of Radiation Oncology, University of Michigan, Ann Arbor, Michigan*
[b] *Department of Nuclear Engineering & Radiological Sciences, University of Michigan, Ann Arbor, Michigan*
[c] *Department of Radiation Oncology, Indiana University, Indianapolis, Indiana*

Received 14 April 2016; received in revised form 13 October 2016; accepted 24 October 2016

Abstract

Purpose: Limits on mean lung dose (MLD) allow for individualization of radiation doses at safe levels for patients with lung tumors. However, MLD does not account for individual differences in the extent or spatial distribution of pulmonary dysfunction among patients, which leads to toxicity variability at the same MLD. We investigated dose rearrangement to minimize the radiation dose to the functional lung as assessed by perfusion single photon emission computed tomography (SPECT) and maximize the target coverage to maintain conventional normal tissue limits.

Methods and materials: Retrospective plans were optimized for 15 patients with locally advanced non-small cell lung cancer who were enrolled in a prospective imaging trial. A staged, priority-based optimization system was used. The baseline priorities were to meet physical MLD and other dose constraints for organs at risk, and to maximize the target generalized equivalent uniform dose (gEUD). To determine the benefit of dose rearrangement with perfusion SPECT, plans were reoptimized to minimize the generalized equivalent uniform functional dose (gEUfD) to the lung as the subsequent priority.

Results: When only physical MLD is minimized, lung gEUfD was 12.6 $\pm$ 4.9 Gy (6.3-21.7 Gy). When the dose is rearranged to minimize gEUfD directly in the optimization objective function, 10 of 15 cases showed a decrease in lung gEUfD of >20% (lung gEUfD mean 9.9 $\pm$ 4.3 Gy, range 2.1-16.2 Gy) while maintaining equivalent planning target volume coverage. Although all dose-limiting constraints remained unviolated, the dose rearrangement resulted in slight gEUD increases to the cord (5.4 $\pm$ 3.9 Gy), esophagus (3.0 $\pm$ 3.7 Gy), and heart (2.3 $\pm$ 2.6 Gy).

Sources of support: This work was supported in part by U.S. National Institutes of Health Grants P01-CA059872 (Ten Haken/Lawrence) and R01-CA142840 (Kong).

Conflicts of interest: None.

* Corresponding author. Department of Radiation Oncology, University of Michigan, 1500 E. Medical Center Drive, SPC 5010, Ann Arbor, MI 48109
E-mail address: marthamm@med.umich.edu (M.M. Matuszak)

http://dx.doi.org/10.1016/j.adro.2016.10.007

Conclusions: Priority-driven optimization in conjunction with perfusion SPECT permits image guided spatial dose redistribution within the lung and allows for a reduced dose to the functional lung without compromising target coverage or exceeding conventional limits for organs at risk.

Introduction

Decades of data collection and analyses of toxicity have helped identify dose-volume metrics and other parameters that describe the probability of radiation-induced normal tissue damage for populations of patients. These efforts have provided, in general, safe normal tissue dose limits and guidance for isotoxic dose escalation protocols.[1-3] However, despite numerous published studies on this topic, the power of dose-volume metrics and mean dose models to predict toxicity in an individual patient are still lacking. This is likely due to the underlying biological differences among patients in a population. The emergence of functional imaging metrics and surrogate biomarkers can further discern the individual risk of a patient and may allow for increased customization of radiation therapy.[4] Several single-institution clinical trials are currently underway to validate these newer modalities, techniques, and metrics.[5]

Established predictors of radiation-induced lung toxicity include dose-volume metrics, mean lung dose (MLD), and normal tissue complication probability models. A summary of accepted models can be found in the Quantitative Analyses of Normal Tissue Effects in the Clinic organ-specific guidance papers.[6] Normal tissue complication probability, for example, has been commonly used as a metric to guide dose-escalation protocols.[1-3] Such models, however, are estimated on the basis of sensitivity for a total population of patients. Thus, their predictive accuracy for individual patients is limited. Furthermore, current dose-volume risk-assessment models treat the whole lung uniformly. This is problematic because patients with non-small cell lung cancer frequently have respiratory comorbidities that result in heterogeneous lung function. Accurate detection of and spatial information on the underlying lung function and distribution are needed both before treatment and early in the course of radiation on an individual patient level.

To further determine the individual risk of radiation-induced lung toxicity, many institutions have studied the use of modalities such as perfusion and ventilation single photon emission computed tomography (SPECT) imaging, inhale and exhale or 4-dimensional computed tomography (CT)-derived ventilation, and more recently Gallium 18-based ventilation and perfusion positron emission tomography and CT.[6-19] These modalities have been used as a way to determine local and overall lung function for assessments of lung viability and treatment response as well as for baseline and adaptive treatment planning. One intuitive use of functional information for treatment planning has been beam angle optimization.[7,8] The use of beams that preferentially spare large areas of well-ventilated or perfused lung has been shown to improve treatment plan evaluation metrics such as mean ventilated lung dose[8] and volumes calculated from dose function histograms based on SPECT intensity[7] compared with plans that use nonoptimized beam directions. Another strategy to minimize the dose to the functional lung is to choose a threshold to represent a functional lung region of interest and minimize the dose to that region in the objective function.[10,15,16,19]

In the prospective setting, choosing beams that preferentially spare the functional lung prior to optimization should be done with caution because it may prioritize functional lung dose minimization over traditional metrics such as physical target, normal tissue dose objectives, and conformity of the target dose. Similarly, contour-based sparing of highly functional regions using a weighted-sum cost function can shift the dose distribution in a way that may sacrifice planning target volume (PTV) coverage, conformity, and/or homogeneity in addition to increasing the radiation dose to other critical organs at risk (OAR).[10,19,20]

To maintain appropriate clinical limits, strict planning guidelines and stepwise planning and evaluation loops are needed.[20] To allow functional image guided treatment planning to become more mainstream and automated, we investigated constrained and prioritized optimization algorithms that allow a strict prioritization of treatment planning goals and controlled tradeoffs with the investigational metric. Instead of a simple weighted-sum cost function or beam orientation optimization, minimizing a functional lung dose objective within a constrained optimization problem ensures that the tradeoffs among target coverage, physical dose metrics, and functional dose minimization are taken into account. This method may even provide improved functional sparing as well as prevent sacrifices made in target coverage or other normal tissue doses due to the removal of potentially useful beams.

Similarly, only minimizing a functional lung objective may be premature. Although functional metrics and defects have shown great promise in predicting lung toxicity,[21-23] large-scale validation is still desirable before phasing out physical dose objectives. The addition of

functional dose-volume objectives to a traditional weighted-sum cost function has been studied by Shioyama et al and St. Hilaire et al., who demonstrated that the addition was beneficial in reducing the dose to the functional lung while preserving other normal tissue limits.[10,24] However, the procedure requires iteration through different cost function weight values or optimization of multiple plans to ensure that the higher priority objectives are not sacrificed. A priority-based optimization strategy such as lexicographic ordering[25] has the advantage of constraining higher priority objectives during optimization so that iteration or backtracking is not required.

The purpose of the current work is to investigate the feasibility of dose rearrangement in normal lung to minimize SPECT functional-volume-weighted lung doses during priority-based inverse planning and maintain constraints on conventional physical dose-volume metrics to maximize target coverage.

Methods and materials

Study population and SPECT/CT scans

Fifteen patients with stage III NCSLC who were previously treated in an institutional review board–approved prospective study on the role of functional imaging in predicting tumor and normal tissue response were randomly selected for retrospective treatment planning. Although patients with an earlier cancer stage were also included in the study, they were excluded from the current investigation to maintain a consistent cohort instead of including patients who were treated with stereotactic body radiation therapy.

As part of the imaging study, perfusion SPECT/CT data were collected within 2 weeks prior to the initiation of treatment. All patients were treated with 3-dimensional conformal radiation therapy with or without chemotherapy. The SPECT/CT data from that study were not used to guide treatment. Perfusion SPECT/CT was performed with a Symbia T6 system (Siemens Medical Solutions, Los Angeles, CA) with the patient immobilized in the treatment position with a standard thorax board. Patients were intravenously administered 185 MBq of Tc-99m-labeled macroaggregated albumin particles prior to scanning. The SPECT scans were obtained with a noncircular orbit and step-and-shoot mode over 360 degrees in 128 frames. The SPECT was reconstructed with a 3-dimensional, ordered subset, expectation-maximization, iterative reconstruction with resolution, scatter, and attenuation correction.

Radiation therapy optimization system

Treatment planning and optimization in this study were performed with software packages developed in-house.[25,26] For beamlet-based IMRT planning, dose calculation points were distributed in volumetric regions of interest based on composite 3-dimensional surfaces that were created from patient contours. Beamlets were defined on a 5 mm × 5 mm grid, although customized beamlet sizes are possible in the software. Dose calculations were run prior to optimization and utilized an in-house convolution superposition algorithm that was commissioned and used clinically. Objective functions could be created using a variety of dose, dose-volume, and biological metrics, including generalized equivalent uniform dose (gEUD).[26] Doses in the optimization system could be displayed as a physical dose or a dose that is corrected to the nominal dose per fraction equivalent using the linear quadratic model (ie, equivalent dose in 2 gray [EQD2] for a 2 Gy per fraction [Gy/Fx] equivalent). Individual objectives (ie, costlets)[26] could also be defined using physical dose or EQD2.

The in-house optimization software allows for 3-dimensional intensity-based functional image data to be incorporated directly in the cost function. To utilize functional images in the cost function, the images must first be registered to the treatment-planning CT dataset. Inside the optimization system, any validated volumetric functional dataset can be activated for use during optimization. When a functional image intensity–based cost function is selected for use in a region of interest, a trilinear interpolation is used to specify the functional image value (ie, intensity) that corresponds to each dose calculation point in the region of interest.

The intensity values can be used directly or normalized based on the average intensity within the region of interest. Optimization of beamlet weights can be performed by either minimizing the weighted sum of all region-specific cost functions with a quasi-newton optimization algorithm or using a priority-based optimization strategy called lexicographic ordering (LO) that utilizes a sequential quadratic programming algorithm with constraints. The LO method, which was utilized in the current work, divides a large optimization problem with many objectives into a series of smaller optimization problems that can be solved sequentially based on their priority in the problem. Our implementation of this method in planning IMRT treatments was discussed in detail by Jee et al.[25]

SPECT-weighted dose metric

The SPECT/CT scans were performed with the same setup and immobilization equipment as the treatment planning CT. Registration between SPECT images and the treatment planning CT was performed via rigid CT-to-CT alignment between each treatment planning CT and the CT of each SPECT/CT. Deformable registration was not applied due to the potential variation in breath-

hold position between the CT from SPECT/CT and the free-breathing SPECT scan. Once aligned, the SPECT/CT transformation was applied to the SPECT dataset(s).

The generalized equivalent uniform functional dose (gEUfD) was used to penalize the dose to the functional lung, which was assumed to be proportional to SPECT intensity and/or signal level, during optimization. The gEUfD as described by Miften et al.[27] is calculated as follows:

$$gEUfD = \left[\frac{\sum_{i=1}^{N} f_i d_i^a}{\sum_{i=1}^{N} f_i}\right]^{1/a} \quad \text{(Eq.1)}$$

where

f_i = SPECT intensity of voxel i in the region of interest (≥ 0)

d_i = dose in voxel i in the region of interest

N = number of voxels in the region of interest

a = region specific parameter

The region of interest used to determine SPECT-weighted gEUfD was defined as both lungs exclusive of the gross tumor volume. Here, the a parameter value was set to 1 to represent the mean value for simplicity. The gEUfD can be computed using perfusion (or ventilation) SPECT intensities. Any saturation artifacts noted on the perfusion scans were thresholded and excluded. However, perfusion images typically avoid artifacts that are similar to those noted on ventilation scans due to aerosol buildup. For gEUfD calculations, the SPECT intensity was normalized with a maximum intensity of 100%.

Priority-based treatment planning and comparisons

To determine the feasibility of redistributing doses based on the minimization of SPECT-weighted gEUfD, new IMRT plans were optimized for the 15 previously treated, randomly selected patients both with and without SPECT gEUfD costlets included in the cost function. All treatment beam angles were picked using standard treatment planning practices with at least 9 beams to provide adequate degrees of freedom to take advantage of dose redistribution.

Table 1 shows the prioritized constrained-optimization goals that were used for inverse planning. All optimizations were performed using LO to ensure that the goals at a higher priority level were not compromised by lower priority objectives. The priority level of 0 constraints was based on standard OAR dose limits that are used in our clinic and in current national protocols. Priority level 1 maximized the PTV generalized equivalent uniform dose (gEUD) up to 75 Gy EQD2 ($\alpha/\beta = 10$ Gy, a = −20) subject to the priority level 0 limits. This metric was chosen to provide a therapeutic dose while allowing some

Table 1 Prioritized objectives for lung intensity modulated radiation therapy with perfusion avoidance

Priority	Structure	Goal	Parameters
0	Cord	Max <50 Gy	EQD2 (α/β = 2.5 Gy)
	Esophagus	gEUD <34 Gy Max <74 Gy	EQD2 (α/β = 10 Gy); a = 1
	Heart	gEUD <30 Gy Max <74 Gy	EQD2 (α/β = 2.5 Gy); a = 1
	Lungs-GTV	gEUD <20 Gy	EQD2 (α/β = 2.5 Gy); a = 1
	PTV	Max <86 Gy	EQD2 (α/β = 10 Gy)
1	PTV	gEUD ≥75 Gy	EQD2 (α/β = 10 Gy); a = −20
2[a]	Lungs-GTV	Minimize gEUfD	EQD2 (α/β = 2.5 Gy); with perfusion SPECT
3	All normal tissues	Minimize dose	EQD2 (α/β = 2.5 Gy)

EQD2, equivalent dose in 2 Gy fractions; gEUD, generalized equivalent uniform dose; gEUfD, generalized equivalent uniform functional dose; GTV, gross tumor volume; PTV, planning target volume; SPECT, single photon emission computed tomography.

[a] Only included in the "Perfusion Avoidance" plans.

heterogeneity in the target region to help facilitate dose rearrangement in the "Perfusion Avoidance" plans. The chosen α/β values are consistent with our clinical practice for early- and late-responding tissues and prior lung and tumor modeling studies.[28,29] To test the effectiveness of the use of perfusion SPECT data, the baseline and "Perfusion Avoidance" objectives deviated for priority level 2. For baseline cases, priority level 2 minimized the dose to all OARs with no additional objectives. To utilize the SPECT data, the "Perfusion Avoidance" cases minimized the gEUfD of the lung at priority level 2 using the perfusion SPECT data. Priority level 3 was then added to minimize the dose to all OARs using the same method as priority level 2 in the baseline cases. The beam arrangement and fluence map resolution were consistent between baseline and perfusion avoidance plans.

To judge the effect that functional avoidance optimization had on PTV homogeneity, the following metric was computed for baseline and perfusion avoidance plans:

$$\text{Homogeneity Metric} = \frac{PTV_{mean1\%} - PTV_{mean99\%}}{PTV_{gEUD}} \quad \text{(Eq.2)}$$

where $PTV_{mean1\%}$ is the mean dose in the hottest 1% of PTV voxels, and $PTV_{mean99\%}$ is the mean dose in the coldest 1% of voxels. A plan conformity metric was also recorded to appreciate the effect of functional avoidance on the conformity of isodose distribution. The conformity metric was defined as:

$$Conformity\ Metric = \frac{Volume_{PTV,gEUD}}{Volume_{PTV}} \quad \text{(Eq.3)}$$

where $Volume_{PTV,gEUD}$ is the volume of the isodose surface that receives at least the gEUD recorded for the PTV. The denominator is simply the volume of the PTV structure.

It should be noted that these gEUD-based conformity values should be judged in a relative manner and that values <1 are not necessarily "worse" but simply represent cases that may have compensated for voxels of lower dose by treating other voxels to much higher doses. Thus, 2 cases could have equivalent gEUDs with one case showing a conformity metric above 1 and the other below 1.

In support of additional plan comparisons, gEUDs for the lung, esophagus, heart, and spinal cord were compared with baseline and functional avoidance plans. The volume of the lung receiving 20 Gy or higher was also recorded. Paired Student *t* tests were performed where appropriate to determine the statistical significance of differences between baseline and functional avoidance plans.

Results

Using the prioritized objectives in Table 1, all plans were optimized to completion per the stages listed with no trial-and-error adjustment of the objective function weights. As such, all "priority 0" normal tissue objectives were met for all plans. The perfusion avoidance plans showed a clear redistribution of dose away from the highly perfused areas of the lung, as expected. Figure 1 shows a typical patient (#8) with baseline and perfusion avoidance dose distributions overlaid on the planning CT and perfusion SPECT scans. The yellow arrows note the areas of redistribution away from the highly perfused lung, and the red arrow highlights an increase in dose to other normal tissues.

Note that for the following results, all dose values are provided in 2 Gy/Fx equivalent or EQD2 with an α/β ratio of 2.5 Gy for the lungs, heart, and spinal cord and 10 Gy for the esophagus and tumor. Quantitatively, when the plan did not account for the lung perfusion distribution (baseline plans), lung gEUfD was on average 12.6 ± 4.9 Gy with a range from 6.3 Gy to 21.7 Gy. When perfusion SPECT data were added at priority level 2 (perfusion avoidance plans), the cases showed decreases in lung gEUfD with an average of 9.9 ± 4.3 Gy and ranged from 2.1 Gy to 16.2 Gy. As shown in Table 2, 10 of 15 cases showed a decrease in gEUfD of at least 20%. The changes in lung gEUfD were statistically significant ($P < .01$) with a paired *t* test.

These data are shown graphically in Figure 2, with the decrease in lung gEUD (equivalent to mean lung dose in EQD2) versus the decrease in lung gEUfD. Although the redistribution resulted in a decrease in non-perfusion-weighted gEUD, the decrease in gEUfD was greater (demonstrated by all values falling below the line). In terms of the lung volume receiving 20 Gy or more, there was also a significant decrease from an average of 20.8 ±

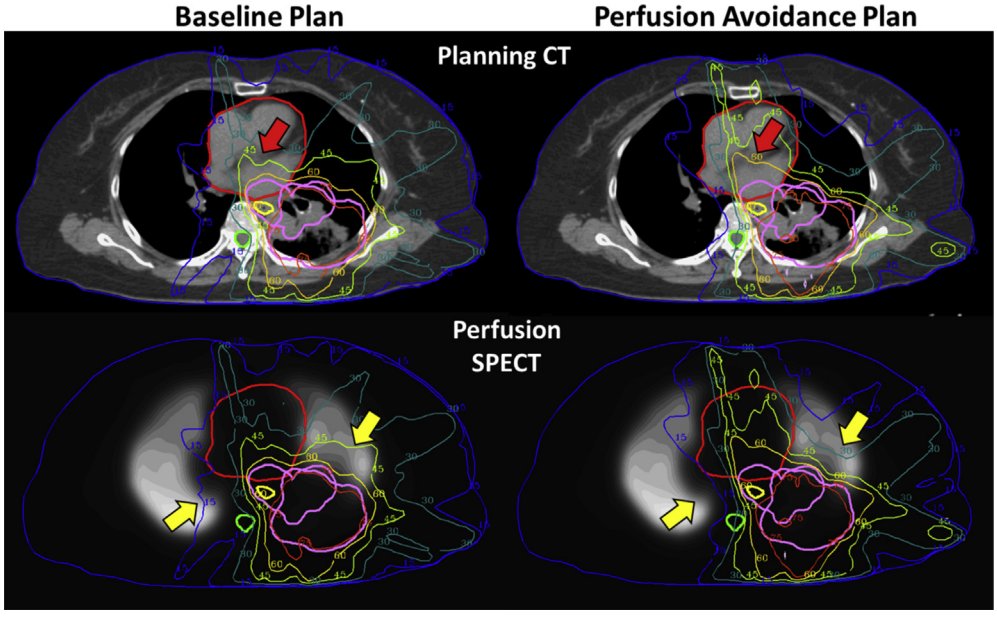

Figure 1 Dose distributions (in absolute physical dose) for the baseline and perfusion avoidance plans displayed on planning computed tomography and perfusion single photon emission computed tomography scans. Yellow arrows denote areas of dose redistribution away from the perfused lung, and the red arrow denotes an increase in heart dose as a result. The heart (thick red contour) mean and maximum dose limits are still met. Planning target volume (PTV) contours for both the nodal and primary PTV are shown in thick pink outlines (PTVs intersect on this slice).

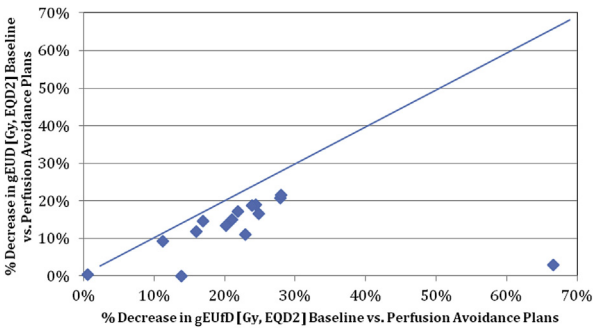

Figure 2 Percent decrease in nonfunctional generalized equivalent uniform dose versus functional dose for the normal lung between baseline and perfusion avoidance plans.

8.6% in baseline plans to 17.3 ± 8.3% in the functional plans ($P < .01$).

Due to the prioritized nature of the optimization, all critical and normal organs that were considered, including the heart, esophagus, and cord, were kept well below the non-negotiable priority level of 0 constraints (Table 1). However, as the dose was redistributed to minimize lung gEUfD, slight increases in the gEUD to other critical organs were observed in the perfusion avoidance plans (Fig 3). Target coverages were rigorously maintained (gEUD = 79.1 ± 1.3 Gy, EQD2 for both baseline and perfusion avoidance plan groups) with slight increases in average gEUD to the spinal cord (5.4 Gy, EQD2), esophagus (3.0 Gy, EQD2), heart (2.3 Gy, EQD2). Although each change was statistically significant ($P < .05$), all metrics were below the priority level of 0 constraints.

PTV homogeneity was very similar ($P = .46$) between baseline and perfusion avoidance plans (Table 3). Using the gEUD objective for PTV, less homogeneity is expected compared with conventional objective functions that strictly ask for minimum and maximum doses in the PTV. The range of homogeneity values is an indication of variability in case geometry and tradeoffs.

The conformity of the dose distribution was significantly reduced in the functional avoidance plans compared with the baseline by an average of 17.6% ($P = .001$). Table 4 shows the conformity metric values by patient. A decrease in conformity can also be noted in the dose distributions for Patient #8 (Fig 1).

Discussion

This study shows that it is feasible to redistribute doses so that doses to the functional lung are lowered and dose constraints in OARs and PTV coverage are maintained. The use of priority-based inverse planning or LO prevents the lesser priority gEUfD minimization objective from violating the normal tissue constraints and already achieved target coverage. In 15 cases that were tested, lung gEUfD was reduced by an average of 22.7% ± 14.1% with the addition of the perfusion based objective. When possible, this type of dose redistribution clearly attempts to push doses away from high SPECT signal strength voxels of the lung and maintain PTV coverage and OAR dose limits.

In practice, this staged dose redistribution strategy will allow us to take the functional imaging data into account to try and minimize functional loss but will not place its priority ahead of maintaining OAR doses at safe levels. In addition, target coverage will not be sacrificed on the basis of the objective as could happen with a priori beam

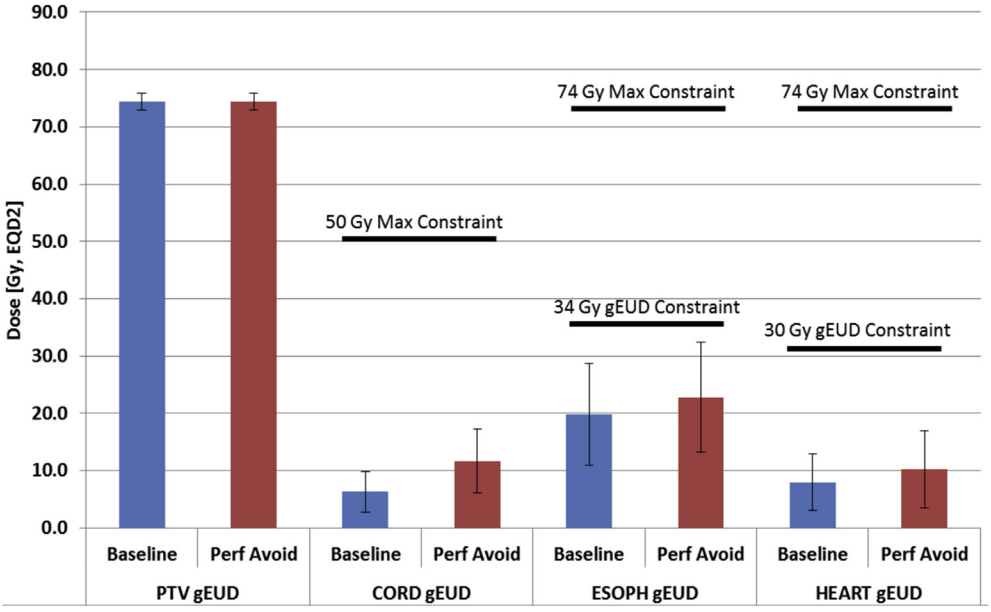

Figure 3 Planning target volume and normal tissue generalized equivalent uniform dose for baseline and functional plans. The priority level with 0 constraints on normal tissues are also denoted.

Table 2 Lung gEUfD for baseline and perfusion avoidance plans (absolute and percent differences for 15 patients with average values)

Patient Number	Lung gEUfD [Gy, EQD2]		Difference	
	Baseline	Perfusion Avoidance	[Gy, EQD2]	[%]
1	6.3	2.1	4.2	66.7
2	17.7	14.7	3.0	16.9
3	14.9	10.7	4.2	27.9
4	12.4	9.5	2.8	22.9
5	14.2	11.1	3.1	21.8
6	9.3	7.0	2.3	24.8
7	8.1	6.4	1.7	21.1
8	15.2	12.2	3.1	20.2
9	8.4	8.4	0.1	0.6
10	21.7	18.2	3.5	16.0
11	6.9	4.9	1.9	28.0
12	12.9	11.1	1.8	13.9
13	8.6	7.6	1.0	11.2
14	10.9	8.2	2.7	24.4
15	21.3	16.2	5.1	23.9
Average	12.6	9.9	2.7	22.7
SD	4.9	4.3	1.3	14.1

EQD2, equivalent dose in 2 Gy fractions; gEUD, generalized equivalent uniform dose; gEUfD, generalized equivalent uniform functional dose.

selection based on SPECT imaging or the incorporation of a functional objective into a traditional weighted-sum cost function, as proposed in other research. Additionally, placing the functional imaging objective into this prioritized optimization technique at a level below conventionally acceptable normal tissue metrics and target coverage assures the user that an optimal plan that meets all protocol objectives is still created. Simply put, for the lung protocol used in our study, optimal, protocol-compliant plans are generated with the same tumor coverage as in baseline optimization but with doses redistributed in the patient on an individualized basis (and particularly within the patient's lungs when possible) to potentially minimize loss of lung function. The application of SPECT intensity-based objective function as opposed to minimization of the dose to a threshold-defined "high perfusion" structure allows the use of a continuous range of perfusion values instead of discretizing. It also benefits from a quick implementation of adaptive therapy because additional contours do not have to be made and added to the objective function.

Table 3 Homogeneity metric for baseline and functional cases

Patient Number	Baseline	Functional	Difference [%]
1	0.24	0.25	2.2
2	0.34	0.33	−0.4
3	0.45	0.45	0.7
4	0.26	0.27	3.7
5	0.28	0.27	−4.0
6	0.27	0.27	−2.1
7	0.28	0.28	−0.1
8	0.28	0.27	−2.5
9	0.48	0.48	0.0
10	0.33	0.32	−1.5%
11	0.29	0.29	0.1%
12	0.31	0.32	2.5%
13	0.25	0.28	12.2%
14	0.27	0.29	6.6%
15	0.27	0.26	−4.3%
Average	0.31	0.31	0.9%
SD	0.07	0.07	4.27

Table 4 Conformity metric for baseline and functional cases

Patient Number	Baseline	Functional	Difference [%]
1	0.92	1.32	43.2
2	1.80	1.86	3.3
3	1.01	1.11	9.9
4	0.74	0.84	13.5
5	0.89	1.09	22.5
6	0.92	1.01	9.8
7	0.86	1.26	46.5
8	0.88	1.05	19.3
9	1.47	1.45	−1.4
10	0.83	0.89	7.2
11	0.68	0.77	13.2
12	0.80	0.89	11.3
13	1.65	2.20	33.3
14	0.81	1.02	25.9
15	0.83	0.88	6.0
Average	1.0	1.2	17.6
SD	0.3	0.4	14.2

Advantages of a priority-based optimization technique with constraints in this setting are a high potential benefit and little risk of reducing plan quality beyond prespecified levels. The added objective in the cost function should only negligibly increase the planning time, and for patients who do not see an appreciable decrease in gEUfD, there is little to no harm in the objective being present in the cost function. With a traditional weighted-sum optimization, the increase in planning time to iterate through weight values of the functional and other objectives may be high with potentially no benefit to the individual patient.

Although our current work focuses on the use of IMRT, the use of volumetric modulated arc therapy (VMAT) is also very common due to the increased delivery efficiency. We are currently investigating the incorporation of more specialized intensity-based objectives into a VMAT algorithm. Given the potentially increased degrees of freedom in the context of entry

angles, VMAT may provide a benefit in functional sparing. We plan to investigate this in future work.

The use of any imaging modality for treatment planning and optimization relies on the suitability of that image for medical decision-making. In the context of functional avoidance, that means that the imaging modality should be reliable and free from any short-term transient changes. Although no studies have been published that explicitly investigate this for perfusion and ventilation SPECT for the lung, this modality is considered to be a reliable tool to diagnose pulmonary conditions.[30] Our group has also observed that non-compromised and unirradiated areas of the lung are consistent on perfusion and ventilation SPECT imaging taken during and after radiation therapy.[14] However, this area may warrant further investigation in the diagnostic community and could affect the uncertainty of functional avoidance regions used in radiation therapy.

Limitations

A limitation of directly using SPECT images for planning is that some regions of the lung are temporarily compromised due to tumor-related effects and could potentially recover during RT treatment. However, if the dose is preferentially distributed in these areas based on pretreatment SPECT imaging, the chance for recovery could be lost. Our institution is currently evaluating how to best identify these potentially recoverable regions so that the SPECT intensity used for planning could be adjusted to better reflect the potential for recovery of function.[14]

Another limitation of the use of SPECT images for dose redistribution is related to how the dose is redistributed. Because one of the highest priorities is to keep tumor coverage high, the perfusion avoidance plans must redistribute the dose to the lung from other OARs to meet this tumor coverage requirement. Due to this, losses in plan conformity and increases in the dose to some OARs were found in nearly all cases studied. Although the increased doses were still considered safe for all OARs, it would be ideal to control this dose increase. Further investigation into this problem would be required, with limitations set on how much the dose to an organ may increase between the baseline and perfusion avoidance cases. With the prioritized optimization strategy, this limit can be applied in a controlled way to an acceptable risk level to other organs.

Finally, we recognize that as more dose response data become available to model the loss of perfusion as a function of dose, more sophisticated optimization objectives will be needed. We are currently analyzing data and developing optimization strategies in both the lung and liver to take advantage of the damage threshold and saturation effects that have been observed. This may entail a functional penalty for the lung that is based on absolute measures of function as opposed to the relative measures that are presented in the current work. The incorporation of improved objectives should fit into the current infrastructure, although updated optimization solvers and methods may be necessary.

Conclusions

Multicriteria LO, with its staged approach to plan objectives, permits the generation of dose-escalated IMRT treatment plans at traditional physical-volume-based levels but with the ability to rearrange doses to minimize ventilation or perfusion SPECT-weighted gEUfD. In a sample of 15 patients, gEUfD was reduced by 22.7% $\pm$ 14.1% when the gEUfD minimization objective was applied. This priority-based spatial dose rearrangement may minimize the dose to the functional lung on an individual level and ultimately minimize long-term radiation-induced lung damage.

References

1. Ten Haken RK, Martel MK, Kessler ML, et al. Use of Veff and iso-NTCP in the implementation of dose escalation protocols. *Int J Radiat Oncol Biol Phys*. 1993;27:689-695.
2. McGinn CJ, Ten Haken RK, Ensminger WD, Walker S, Wang S, Lawrence TS. Treatment of intrahepatic cancers with radiation doses based on a normal tissue complication probability model. *J Clin Oncol*. 1998;16:2246-2252.
3. Hayman JA, Martel MK, Ten Haken RK, et al. Dose escalation in non-small-cell lung cancer using 3-dimensional conformal radiation therapy: update of a phase I trial. *J Clin Oncol*. 2001;19:127-136.
4. Das SK, Ten Haken RK. Functional and molecular image guidance in radiotherapy treatment planning optimization. *Semin Radiat Oncol*. 2011;21:111-118.
5. ClinicialTrials.gov. Clinicaltrials.gov Online Search "Functional Imaging Lung Radiotherapy". Available at: https://clinicaltrials.gov/ct2/results?term=lung+functional+imaging+radiotherapy&Search=Search. Accessed October 2016.
6. Marks LB, Bentzen SM, Deasy JO, et al. Radiation dose-volume effects in the lung. *Int J Radiat Oncol Biol Phys*. 2010;76:S70-S76.
7. McGuire SM, Marks LB, Yin FF, Das SK. A methodology for selecting the beam arrangement to reduce the intensity-modulated radiation therapy (IMRT) dose to the SPECT-defined functioning lung. *Phys Med Biol*. 2010;55:403-416.
8. Munawar I, Yaremko BP, Craig J, et al. Intensity modulated radiotherapy of non-small-cell lung cancer incorporating SPECT ventilation imaging. *Med Phys*. 2010;37:1863-1872.
9. Marks LB, Spencer DP, Bentel GC, et al. The utility of SPECT lung perfusion scans in minimizing and assessing the physiologic consequences of thoracic irradiation. *Int J Radiat Oncol Biol Phys*. 1993;26:659-668.
10. Shioyama Y, Jang SY, Liu HH, et al. Preserving functional lung using perfusion imaging and intensity-modulated radiation therapy for advanced-stage non-small cell lung cancer. *Int J Radiat Oncol Biol Phys*. 2007;68:1349-1358.

11. Zhang J, Ma J, Zhou S, et al. Radiation-induced reductions in regional lung perfusion: 0.1-12 year data from a prospective clinical study. *Int J Radiat Oncol Biol Phys*. 2010;76:425-432.
12. De Jaeger K, Seppenwoolde Y, Boersma LJ, et al. Pulmonary function following high-dose radiotherapy of non-small-cell lung cancer. *Int J Radiat Oncol Biol Phys*. 2003;55:1331-1340.
13. Marks LB, Munley MT, Spencer DP, et al. Quantification of radiation-induced regional lung injury with perfusion imaging. *Int J Radiat Oncol Biol Phys*. 1997;38:399-409.
14. Yuan S, Frey KA, Gross MD, et al. Semiquantification and classification of local pulmonary function by V/Q single photon emission computed tomography in patients with non-small cell lung cancer: Potential indication for radiotherapy planning. *J Thor Oncol*. 2011; 6:71-78.
15. Christian JA, Partridge M, Nioutsikou E, et al. The incorporation of SPECT functional lung imaging into inverse radiotherapy planning for non-small cell lung cancer. *Radiother Oncol*. 2005; 77:271-277.
16. Bates EL, Bragg CM, Wild JM, Hatton MQ, Ireland RH. Functional image-based radiotherapy planning for non-small cell lung cancer: A simulation study. *Radiother Oncol*. 2009;93:32-36.
17. Lavrenkov K, Singh S, Christian JA, et al. Effective avoidance of a functional spect-perfused lung using intensity modulated radiotherapy (IMRT) for non-small cell lung cancer (NSCLC): An update of a planning study. *Radiother Oncol*. 2009;91:349-352.
18. Siva S, Callahan J, Kron T, et al. A prospective observational study of Gallium-68 ventilation and perfusion PET/CT during and after radiotherapy in patients with non-small cell lung cancer. *BMC cancer*. 2014;14:740.
19. Yaremko BP, Guerrero TM, Noyola-Martinez J, et al. Reduction of normal lung irradiation in locally advanced non small cell lung cancer patients using ventilation images for functional avoidance. *Int J Radiat Oncol Biol Phys*. 2007;68:562-571.
20. Yamamoto T, Kabus S, von Berg J, Lorenz C, Keall PJ. Impact of 4-dimensional computed tomography pulmonary ventilation imaging-based functional avoidance for lung cancer radiotherapy. *Int J Radiat Oncol Biol Phys*. 2011;79:279-288.
21. Ebert N, Baumann M, Troost EG. Radiation-induced lung damage - Clinical risk profiles and predictive imaging on their way to risk-adapted individualized treatment planning? *Radiother Oncol*. 2015;117:1-3.
22. Gayed IW, Chang J, Kim EE, et al. Lung perfusion imaging can risk stratify lung cancer patients for the development of pulmonary complications after chemoradiation. *J Thor Oncol*. 2008;3: 858-864.
23. Vinogradskiy Y, Castillo R, Castillo E, et al. Use of 4-dimensional computed tomography-based ventilation imaging to correlate lung dose and function with clinical outcomes. *Int J Radiat Oncol Biol Phys*. 2013;86:366-371.
24. St-Hilaire J, Lavoie C, Dagnault A, et al. Functional avoidance of lung in plan optimization with an aperture-based inverse planning system. *Radiother Oncol*. 2011;100:390-395.
25. Jee KW, McShan DL, Fraass BA. Lexicographic ordering: intuitive multicriteria optimization for IMRT. *Phys Med Biol*. 2007;52:1845-1861.
26. Kessler ML, McShan DL, Epelman MA, et al. Costlets: A generalized approach to cost functions for automated optimization of IMRT treatment plans. *Optim Eng*. 2005;6:421-448.
27. Miften MM, Das SK, Su M, Marks LB. Incorporation of functional imaging data in the evaluation of dose distributions using the generalized concept of equivalent uniform dose. *Phys Med Biol*. 2004;49:1711-1721.
28. Guckenberger M, Klement RJ, Allgauer M, et al. Local tumor control probability modeling of primary and secondary lung tumors in stereotactic body radiotherapy. *Radiother Oncol*. 2016;118:485-491.
29. Seppenwoolde Y, Lebesque JV, de Jaeger K, et al. Comparing different NTCP models that predict the incidence of radiation pneumonitis. Normal tissue complication probability. *Int J Radiat Oncol Biol Phys*. 2003;55:724-735.
30. Clemens S, Leeper KV Jr. Newer modalities for detection of pulmonary emboli. *Am J Med*. 2007;120:S2-S12.